Experimental Hematology

Experimental Hematology 2019;71:51–60

Human iPSC-based model of severe congenital neutropenia reveals elevated UPR and DNA damage in CD34$^+$ cells preceding leukemic transformation

Benjamin Dannenmann[a], Azadeh Zahabi[a], Perihan Mir[a,b], Benedikt Oswald[a], Regine Bernhard[a], Maksim Klimiankou[a], Tatsuya Morishima[a], Klaus Schulze-Osthoff[b,c], Cornelia Zeidler[d], Lothar Kanz[a], Nico Lachmann[e], Thomas Moritz[e], Karl Welte[f], and Julia Skokowa[a]

[a]*Department of Oncology, Hematology, Immunology, Rheumatology, and Pulmonology, University Hospital Tuebingen, Tuebingen, Germany;* [b]*German Cancer Research Center (DKFZ), Heidelberg, Germany;* [c]*Interfaculty Institute of Biochemistry, Tübingen University, Germany;* [d]*Department of Hematology, Oncology, and Bone Marrow Transplantation, Hannover Medical School, Hannover, Germany;* [e]*Institute of Experimental Hematology, Hannover Medical School, Hannover, Germany;* [f]*University Children's Hospital Tuebingen, Tuebingen, Germany*

(Received 10 October 2018; revised 23 December 2018; accepted 30 December 2018)

We describe the establishment of an embryoid-body-based protocol for hematopoietic/myeloid differentiation of human induced pluripotent stem cells that allows the generation of CD34$^+$ cells or mature myeloid cells in vitro. Using this model, we were able to recapitulate the defective granulocytic differentiation in patients with severe congenital neutropenia (CN), an inherited preleukemia bone marrow failure syndrome. Importantly, in vitro maturation arrest of granulopoiesis was associated with an elevated unfolded protein response (UPR) and enhanced expression of the cell cycle inhibitor p21. Consistent with this, we found that CD34$^+$ cells of CN patients were highly susceptible to DNA damage and showed diminished DNA repair. These observations suggest that targeting the UPR pathway or inhibiting DNA damage might protect hematopoietic cells of CN patients from leukemogenic transformation, at least to some extent.

Severe congenital neutropenia (CN) is a monolineage preleukemia bone marrow failure syndrome characterized by early onset of neutropenia and severe infections due to promyelocytic maturational arrest in the bone marrow [1,2]. CN is a heterogeneous disease caused by mutations in a number of genes, including *ELANE* [3] (the most common [1]), *HAX1* [4], *CSF3R* [5,6], *JAGN1* [7], *G6PC3* [8], *TCIRG1* [9], and others. In most cases, *ELANE* mutations are missense mutations that are distributed throughout all five exons of the ELANE gene, although a majority of mutations are found in exons 4 and 5 [10]. Hematopoietic stem and progenitor cells (HSPCs) of CN patients (CN-HSPCs) fail to differentiate into neutrophilic granulocytes, but show no severe maturation defects in other blood lineages [1,2,11,12]. Exposure of CN-HSPCs to high concentrations of granulocyte colony-stimulating factor (G-CSF) partially reverses granulocytic maturation defects [1,12], but approximately 10% of CN patients do not respond to G-CSF doses up to 50 μg/kg/d. The mechanism underlying the granulocytic differentiation defects in bone marrow HSPCs of CN patients has only been partially elucidated. Among the relevant factors, we have identified deregulated levels of LEF-1 [13,14], C/EBPα [13], and PU.1 [15,16] transcription factors; hyperactivated JAK2 [17] and phospho-STAT5a [18]; elevated NAMPT/SIRT1 signaling [19]; abrogated expression of the anti-apoptotic genes Bcl2 and Bcl-xl [20], and markedly diminished expression of the natural inhibitor of neutrophil proteases SLPI (secretory leukocyte protease inhibitor) [21]. In addition, we and others have shown that mutant neutrophil elastase (NE) triggers activation of the unfolded protein response (UPR) and induction of endoplasmic reticulum (ER) stress caused by accumulation of altered (incompletely

Offprint requests to: Prof. Julia Skokowa, Department of Oncology, Hematology, Immunology, Rheumatology and Pulmonology, University Hospital Tuebingen, Otfried-Müller-Str. 10, Tübingen D-72076, Germany; E-mail: julia.skokowa@med.uni-tuebingen.de

0301-472X/
https://doi.org/10.1016/j.exphem.2018.12.006

folded or misfolded) NE protein within the ER or by disturbed intracellular trafficking of NE [22–24].

Despite these insights, we are still far from a clear understanding of the ultimate origin of the defective granulopoiesis and leukemic transformation in CN. There are no animal models of CN, except for rare neutropenia cases caused by inherited mutations in *GFI1* (growth factor independent 1). *Elane*$^{-/-}$ and *Hax1*$^{-/-}$ mice, as well as transgenic mice with a knock-in of a human *ELANE* mutation [23], exhibit normal hematopoietic phenotypes and are not neutropenic. Reprogramming somatic cells of CN patients into induced pluripotent stem cells (iPSCs), followed by hematopoietic differentiation of iPSCs, provides a means for establishing an in vitro model of neutropenia and leukemic transformation in CN. iPSC hematopoietic differentiation models have limitations and cannot fully replace in vivo mouse disease models, but they represent an excellent source of immature hematopoietic cells and mature myeloid cells for further experimentation. Generation of CN-patient-specific iPSCs that recapitulate the maturation arrest of granulopoiesis has been described previously [25–28].

In the present study, we describe the establishment of an experimental in vitro model for studying CN using patient-derived iPSCs. Using this model, we were able to identify upregulation of key components of the UPR pathway and enhanced DNA damage and increased p21 protein levels in CD34$^+$ cells and CD45$^+$ cells of CN patients.

Methods

iPSC cell culture

iPSCs were maintained on mitomycin-C-treated SNL-feeder cells (Public Health England, GB) in iPSC medium consisting of DMEM F12 (Sigma-Aldrich, Germany) supplemented with 20% Knockout Serum Replacement (Invitrogen, USA), 30 ng/mL basic fibroblast growth factor (bFGF; Peprotech, USA), 1% nonessential amino acid solution (Invitrogen, USA), 100 μmol/L 2-mercapto-ethanol, and 2 mmol/L L-glutamine. iPSC medium was replaced every day. hiPSCs were subcultured by manual colony picking on new SNL feeder cells every 10 days.

Reprogramming of peripheral blood mononuclear cells

A total of 1.5×10^6 peripheral blood mononuclear cells were cultured after thawing for 6 days in CD34$^+$ cell expansion medium (Stemline II Medium, Sigma-Aldrich, Germany) supplemented with 10% fetal calf serum, 1% penicillin/streptomycin, 1% glutamine, and the following cytokines: interleukin-3 (IL-3; 20 ng/μL), IL-6 (20 ng/μL), thrombopoietin (20 ng/μL), stem cell factor (SCF; 50 ng/μL), and FLT3L (50 ng/μL). All cytokines were purchased from R&D Systems (USA). After 1 week, cells were added to Retronectin (Clontech, USA)-coated 12-well plates together with OSKM lentiviral supernatant (pRRL.PPT.SF.hOct34.hKlf4.hSox2.i2dTomato.pre.FRT, provided by A. Schambach) with multiplicity of infection of 2. Four days later, cells were transferred to SNL feeders and cultured in an 1:1 mixture of iPSC medium and CD34$^+$ cell expansion medium supplemented with 2 mmol/L valproic acid and 50 μg/mL vitamin C. Medium was gradually changed to iPSC medium only. The first iPSC colonies appeared approximately 3 weeks after initiation of reprogramming.

Quantitative reverse transcription polymerase chain reaction

For quantitative reverse transcription polymerase chain reaction (qRT-PCR), RNA was isolated using RNeasy Micro Kit (Qiagen, Germany). cDNA was prepared from 1 μg of total RNA using the Omniscript RT Kit (Qiagen, Germany). qRT-PCR was performed using SYBR Green qPCR Master Mix (Roche, Switzerland) on Light Cycler 480 (Roche). Data were analyzed using the ddCT method. Target genes were normalized to *GAPDH* and *ACTB* as housekeeper genes. qRT-PCR primer sequences are listed in Supplementary Table E1 (online only, available at www.exphem.org).

Western blotting

A total of 1×10^6 cells were lysed in 200 μL of 3 × Laemmli buffer. Protein was denaturated for 10 min at 95°C. Then, 5 μL of cell lysate in Laemmli buffer was loaded per lane. Proteins were separated on a 12% polyacrylamide gel and transferred on a nitrocellulose membrane (GE Healthcare, USA) for 1 hour at 100 V and 4°C. Membrane was blocked for 1 hour in 5% bovine serum albumin (BSA)/Tris-buffered saline + Tween 20 and incubated in primary antibody overnight at 4°C. The following primary antibodies were used: anti-p21 (Cell Signaling Technology, #2947S), anti-CHOP (Cell Signaling Technology, #2895S), and anti-NE (Santa Cruz Biotechnology, sc-55549) and anti-β-actin (Cell Signaling Technology, #13E5). Next, membranes were washed and incubated with secondary horseradish peroxidase-coupled (Santa Cruz Biotechnology) antibody for 1 hour at room temperature. Enhanced chemoluminescence solution (Thermo Fisher Scientific, USA) and Amersham Hyperfilm were used to detect chemiluminescence signal of proteins.

Embryoid-body-based hematopoietic differentiation of iPSCs

iPSCs were dissociated from SNL feeders or Matrigel (Corning, USA)-coated plates using phosphate-buffered saline (PBS)/ethylenediaminetetraacetic acid (0.02%) for 5 min. Embryoid body (EB) generation was done via centrifugation of 20,000 cells per EB in 96-well plates using APEL serum-free differentiation medium (StemCell Technologies, Canada) supplemented with bFGF (20 ng/μL) and Rho kinase (ROCK) inhibitor (10 μmol/L) (R&D Systems). The next day, bone morphogenetic protein 4 (BMP4; 20 ng/μL) was added to the culture to induce mesodermal differentiation. On day four, EBs were plated on Matrigel-coated six-well plates (10 EBs/well) in APEL medium supplemented with vascular endothelial growth factor (VEGF; 40 ng/μL), SCF (50 ng/μL), and IL-3 (50 ng/μL). For neutrophilic differentiation, medium was changed 3 days later to fresh APEL medium supplemented with IL-3 (50 ng/μL) and G-CSF (50 ng/μL). The first hematopoietic suspension cells appeared on day 12 to day 14.

Suspension cells were harvested every 3–4 days and analyzed starting from day 14 to day 32. All cytokines were purchased from R&D Systems if not otherwise indicated.

Flow cytometry

A total of 30,000 suspension cells collected from an EB-based hematopoietic differentiation system were used for flow cytometry. For cell surface staining, cells were prepared in PBS/1% BSA containing 0.05% sodium azide and stained with the mouse monoclonal antihuman antibody. For detection of mature myeloid cells, a multicolor fluorescence-activated cell-sorting (FACS) antibody panel for "late-stage" hematopoietic differentiation using the following antibodies was applied: CD15-PE, CD16-FITC, CD14-APC-H7, CD45-BV510, CD33-BV421, CD11b-PE-Cy7, and 7-AAD. Samples were analyzed using a FACSCanto II (BD Biosciences, Germany) and FlowJo version 10 software. Antibodies for flow cytometry were purchased from BD Biosciences if not otherwise indicated.

Morphological analysis

Wright–Giemsa-stained cytospin slides were prepared using Hema-Tek slide stainer (LabX, Canada). Hematopoietic cells were classified into four groups according to the differentiation state: myeloblast and promyelocyte (MB/ProM), myelocyte and metamyelocyte (Myelo/Meta), band and segmented neutrophils (Band/Seg), and monocytes/macrophages (Mo/MΦ).

DNA damage quantification

A total of 2.5×10^4 iPSC-derived $CD34^+/CD45^+$ cells were resuspended in PBS and treated with the indicated concentrations of bleomycin for 5 min at room temperature. Genomic DNA was isolated using the QIAamp DNA Mini Kit (Qiagen, Germany). Long-run real-time PCR-based DNA-damage quantification (LORD-Q) was performed and analyzed according to Lehle et al. [29].

Statistical analysis

Differences in mean values between groups were analyzed using two-sided, unpaired Student *t* tests using the SPSS (IBM, USA) version 9.0 statistical package.

Results

In vitro EB-based iPSC differentiation model reveals severely impaired myelopoiesis of CN and CN/acute myeloid leukemia patient-derived iPSCs

We generated iPSCs from two *ELANE*-CN patients, one patient with p.C151Y (CN1), and another patient with p.G214R (CN2) *ELANE* mutations. From one CN patient, we were able to generate iPSC clones harboring either an *ELANE* p.C151Y mutation only (CN-iPSC clone) or additional *CSF3R* and *RUNX1* mutations and trisomy 21 (CN/acute myeloid leukemia [AML]-iPSC clone). All iPSC lines expressed elevated protein and mRNA levels of pluripotent stem-cell-specific factors and showed inactivation of the lentiviral plasmid used for reprogramming.

To evaluate myeloid differentiation of *ELANE*-CN patients iPSCs, we slightly modified an in vitro EB-based iPSC differentiation method developed by Lachmann et al. [30] that allows generation of hematopoietic cells and mature myeloid cells for more than 30 days. EB formation was performed by first centrifuging dissociated iPSCs (20,000 cells/EB) in 96-well conical-bottomed plates in APEL serum-free differentiation medium containing bFGF and ROCK inhibitors, followed by induction of mesodermal differentiation by the addition of BMP4 on day 1 of culture. To induce hematopoietic differentiation, we plated EBs on Matrigel-coated six-well plates (10 EBs/well) in APEL medium supplemented with VEGF, SCF, and IL-3 on day 4 of culture. Neutrophilic differentiation was initiated 3 days later by replacement of cytokines with IL-3 and G-CSF (Figure 1A). In EBs cultured from healthy donor (HD)-derived iPSCs, hematopoietic cells appeared in the supernatants on day 14 and the number of cells was markedly increased at day 28 of culture (Figure 1B). In contrast, the number of hematopoietic cells in culture supernatants of EBs from CN patient-derived iPSCs was markedly diminished and almost no myeloid cells were produced from cultured CN/AML iPSCs (Figure 1B). Consistent with these observations, granulocytic differentiation into mature polymorphonuclear neutrophils ($CD15^+CD16^+CD45^+$ cell population) was markedly reduced in iPSC lines of both *ELANE*-CN patients compared with HD-derived iPSCs and was abolished in CN/AML-iPSCs (Figure 1C). However, the number of monocytes ($CD14^+$ $CD11b^+CD45^+$ cells) produced by CN patient-derived iPSCs was strongly increased compared with that produced by HD-derived iPSCs (Figure 1C). This pattern recapitulates the situation in CN patients, in whom monocyte numbers in the peripheral blood are elevated [31]. Morphological examinations of Giemsa-stained cytospin slides confirmed these results (Figure 1D). Therefore these observations demonstrate the successful establishment of an in vitro model to evaluate mechanisms of diminished granulocytic differentiation of hematopoietic cells in CN patients.

Elevated ER stress and UPR in $CD34^+$ and $CD45^+$ cells from CN patient- and CN1/AML patient-derived iPSCs

We next investigated whether intracellular signaling pathways operating during induction of the UPR, which is known to be hyperactivated in primary HSPCs and granulocytes of CN patients [21–24], are also affected in iPSC-derived hematopoietic cells. We found that *ELANE* mRNA and NE protein levels were highly upregulated in $CD34^+$ cells generated from CN1/AML-iPSCs compared with those generated from CN-iPSCs and HD-iPSCs (Figures 2A and 2C). We detected deregulation of mRNA expression of the UPR downstream targets in CN1 and CN2 iPSC-derived $CD34^+$ cells. Therefore DDIT3 (DNA-

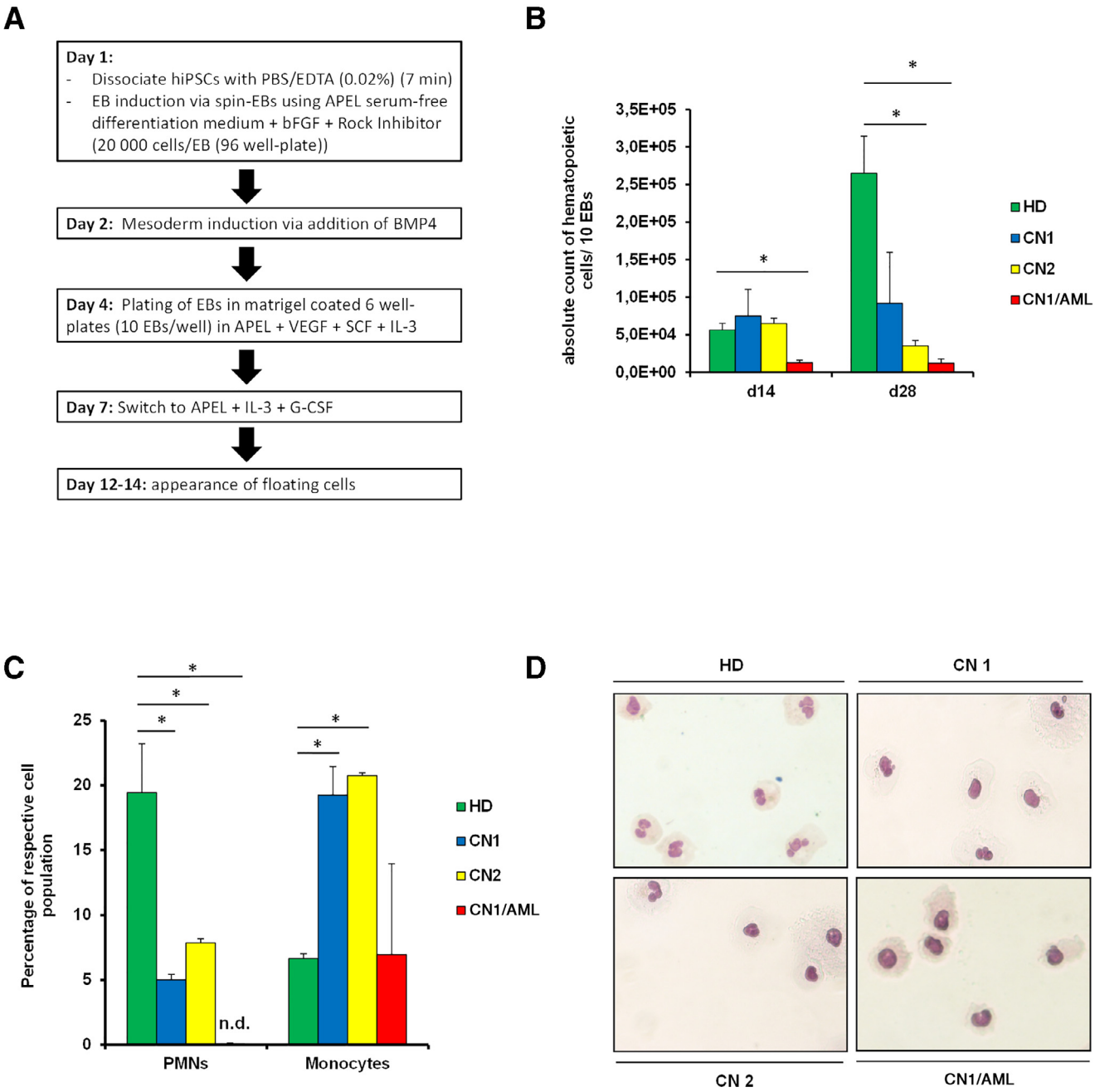

Figure 1. In vitro model of CN and CN/AML using EB-based myeloid differentiation method of patients iPSCs. **(A)** Scheme of the protocol for EB-based hematopoietic and neutrophilic differentiation of iPSCs. **(B)** Production of hematopoietic cells from iPSCs over time in the EB-based differentiation system. Hematopoietic cells were harvested from EB culture supernatants starting from day 14 to day 28 and counted using trypan blue dye exclusion. Data represent means ± SD from two independent experiments. Two-sided, unpaired Student *t* test *p* values to HD are shown. $*p < 0.05$. **(C)** Flow cytometry analysis of suspension cells harvested from EBs culture on day 28 of differentiation. Data represent means ± SD from two independent experiments. $*p < 0.05$. **(D)** Morphological analysis of suspension cells harvested from iPSCs at day 28 of differentiation (Wright-Giemsa Stain). Representative cytospin slide pictures are shown. *HD*, healthy donor.

damage inducible transcript 3, also called CHOP) was increased in $CD34^+$ cells generated from CN1-iPSCs, CN2-iPSCs, and CN1/AML-iPSCs compared with those from HD-iPSCs (Figure 2B). In contrast, expression of mRNA for BiP (binding immunoglobulin protein) was upregulated in CN2, but not CN1-iPSC- or CN1/AML-iPSC-derived $CD34^+$ cells. ATF6 (activating transcription factor 6) mRNA was highly expressed in $CD34^+$ cells derived from CN1-iPSCs, but not in CN2-iPSC- or CN1/AML-iPSC-derived cells. In contrast, maximum ATF4 (activating transcription factor 4) mRNA expression was detected in $CD34^+$ cells from CN2-iPSCs and CN1/AML-iPSCs, but

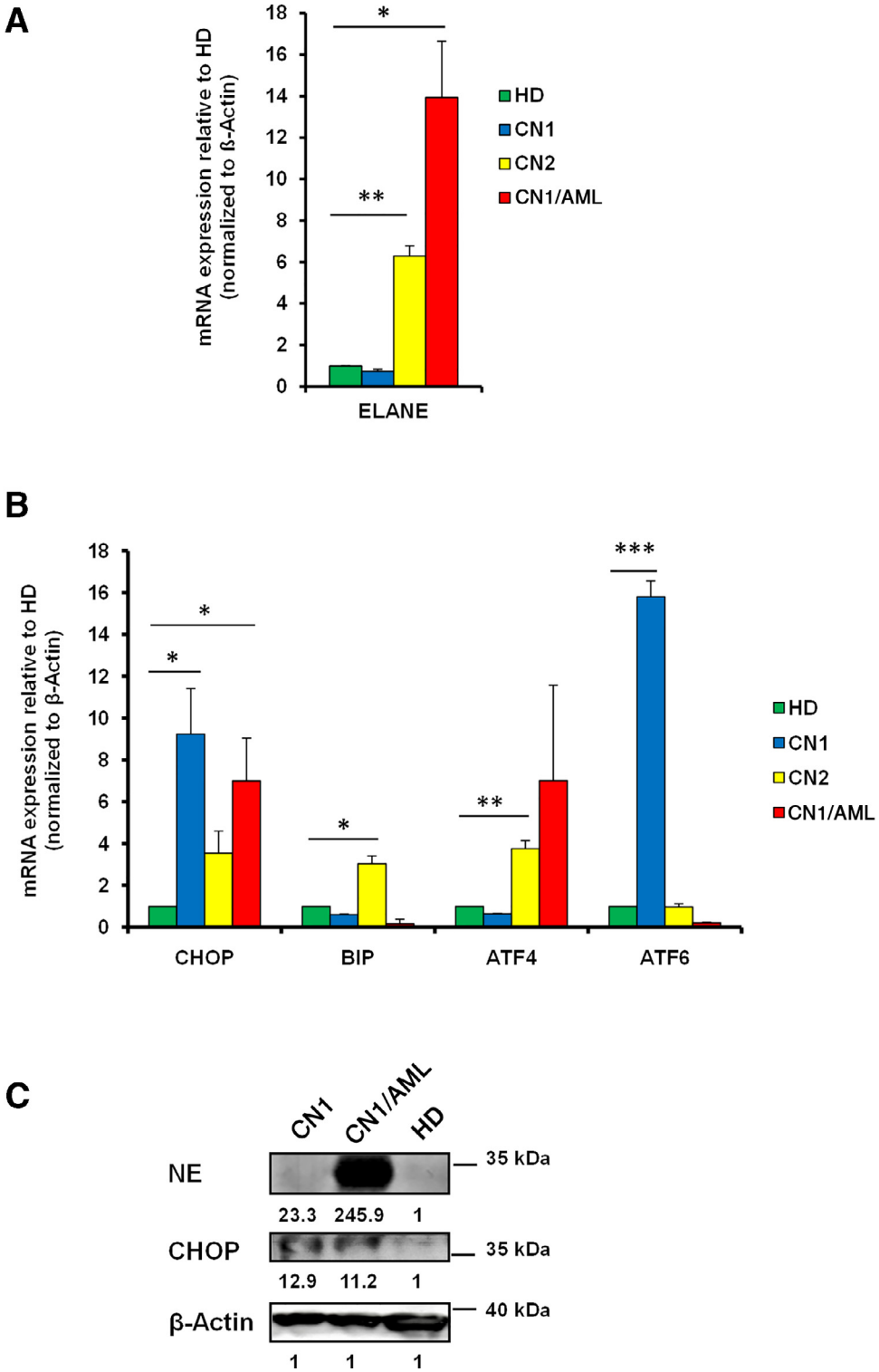

Figure 2. Analysis of ER stress and unfolded protein response (UPR) in $CD34^+$ and $CD45^+$ cells derived from CN- and CN/AML-iPSCs. **(A)** qRT-PCR analysis of ELANE mRNA expression in $CD45^+CD34^+$ cells at day 14 of iPSC differentiation. Data represent means ± SD from two independent experiments. *$p < 0.05$, **$p < 0.001$. **(B)** qRT-PCR analysis of mRNA expression of UPR-related genes in $CD45^+CD34^+$ cells at day 14 of iPSC differentiation, as indicated. Data represent means ± SD from two independent experiments. *$p < 0.05$, **p <0.01, ***$p < 0.001$. **(C)** Representative Western blot images of NE and CHOP protein expression in $CD45^+$ cells at day 28 of iPSC differentiation, as indicated. Numbers below Western blot images indicate protein expression levels normalized to β-Actin.

not in those from CN1-iPSCs or HD-iPSCs (Figure 2B). CHOP protein levels were also elevated in $CD45^+$ cells derived on day 28 of EB differentiation of CN and CN/AML iPSCs (Figure 2C).

DNA damage and DNA-repair responses in $CD34^+$ cells from CN-iPSCs

We further assessed whether elevated ER stress resulting from UPR sensitizes CN-iPSC-derived $CD34^+$ cells to DNA damage. DNA damage was induced by treating cells with bleomycin for 5 min, after which bleomycin was removed and DNA damage and DNA repair were assessed immediately and after 2 hours of incubation (Figure 3A). Long-run, real-time PCR-based DNA-damage quantification (LORD-Q [29]) of genomic DNA loci (*GAPDH* and *TP53*) and mitochondrial DNA (mtDNA) revealed a robust increase in mtDNA and nuclear DNA lesions in CN-iPSC-derived $CD34^+$ cells compared with HD-iPSC-derived cells (Figure 3B). Damaged mtDNA and GAPDH DNA loci, but not *TP53* DNA loci, were also more frequent in $CD34^+$ cells from CN-iPSCs 2 hours after bleomycin treatment compared with that in HD-iPSC-derived $CD34^+$ cells. These data suggest delayed DNA repair and increased susceptibility to DNA damage in $CD34^+$ cells from CN-iPSC lines (Figure 3C).

p21 upregulation in $CD34^+$ and $CD45^+$ cells from CN-iPSCs and CN/AML-iPSCs

We next sought to determine whether DNA damage pathways are differentially regulated in $CD34^+$ and $CD45^+$ cells generated from iPSCs of CN or CN/AML patients compared with HD-generated cells. Our assessment of the role of the p53-p21 pathway, which is typically activated upon DNA damage, showed no differences in *TP53* mRNA expression, but revealed an approximately threefold increase in p21 mRNA expression in CN-iPSC-derived blood cells compared with those derived from HD cells and a fivefold to sixfold increase in CN/AML-iPSC-derived cells (Figure 3D). p21 protein levels were also elevated in CN/AML cells (Figure 3E). The expression of MDM2 mRNA was markedly diminished in CN/AML cells, and GADD45a mRNA expression was slightly induced in both CN-iPSC- and CN/AML-iPSC-derived cells compared with those derived from HD-iPSCs (Figure 3D). Interestingly, p21 mRNA expression was also upregulated in primary bone marrow $CD33^+$ cells of CN patients compared with those of G-CSF-treated healthy individuals, in which p21 levels were even suppressed by G-CSF (data not shown).

Discussion

In the present study, we established an in vitro model of CN using patient-derived iPSCs. We also successfully reprogrammed AML blasts from one CN/AML patient and were able to compare hematopoietic and myeloid differentiation of iPSCs derived from CN/AML cells, CN patients, and a healthy donor. Our data provide strong evidence that, despite some limitations, iPSCs represent a valuable resource for disease modeling, especially for investigations on inherited bone marrow failure syndromes. Primary bone marrow material from pediatric patients with bone marrow failure is extremely limited and mouse models are not available for many of these syndromes. In this latter context, *elane*$^{-/-}$ mice, *hax1*$^{-/-}$ mice, and transgenic mice carrying mutated *elane* do not exhibit neutropenia. In addition, transgenic mice carrying a truncated G-CSF receptor (*csf3r*) mutant never develop leukemia. These acquired *CSF3R* mutations are observed in leukemic blasts of more than 80% of CN patients with overt AML or MDS [32].

Using our iPSC model, we were able to recapitulate the hematopoietic and myeloid differentiation defects of HSPCs observed in CN patients in vivo. Specifically, we detected diminished granulocytic differentiation of CN-iPSCs, an observation consistent with the induction of UPR. iPSC lines from two CN patients showed different behavior during first 2 weeks of hematopoietic differentiation, when differentiation of EBs into $CD34^+$ $CD45^+$ cells occurs, but both CN patients' iPSC lines demonstrated similar markedly diminished granulocytic differentiation at later stages. These early differentiation stage differences may be explained by the varying effects of the mutated NE protein on blood cell formation, which is dependent on the mutated amino acid residues. Interestingly, different *ELANE* mutations resulted in abolished granulocytic differentiation of CN patient-derived iPSCs, an observation consistent with insights gained from CN patients [1]. Monocytic differentiation was elevated in CN-iPSC lines, an observation that parallels the common finding of peripheral blood monocytosis in CN patients [1,31]. One possible explanation for this monocytosis is a compensatory reaction of the bone marrow to diminished neutrophil counts and function that serves to induce an immune response to bacterial pathogens. An alternative explanation is deregulated expression of lineage-specific (granulocyte-specific vs. monocyte-specific) transcription factors in myeloid progenitor cells of CN patients. Deregulated expression of relevant transcription factors (e.g., diminished expression of LEF-1 and C/EBPα, but elevated PU.1 expression) has been described by us previously [15]. Elevated monocytic maturation of CN patients' iPSC lines in vitro further supports the theory that deregulation of a transcriptional program in HSPCs is a cause of neutropenia and monocytosis.

UPR hyperactivation in primary HSPCs of CN patients has been described previously [22–24]. It is presumed that

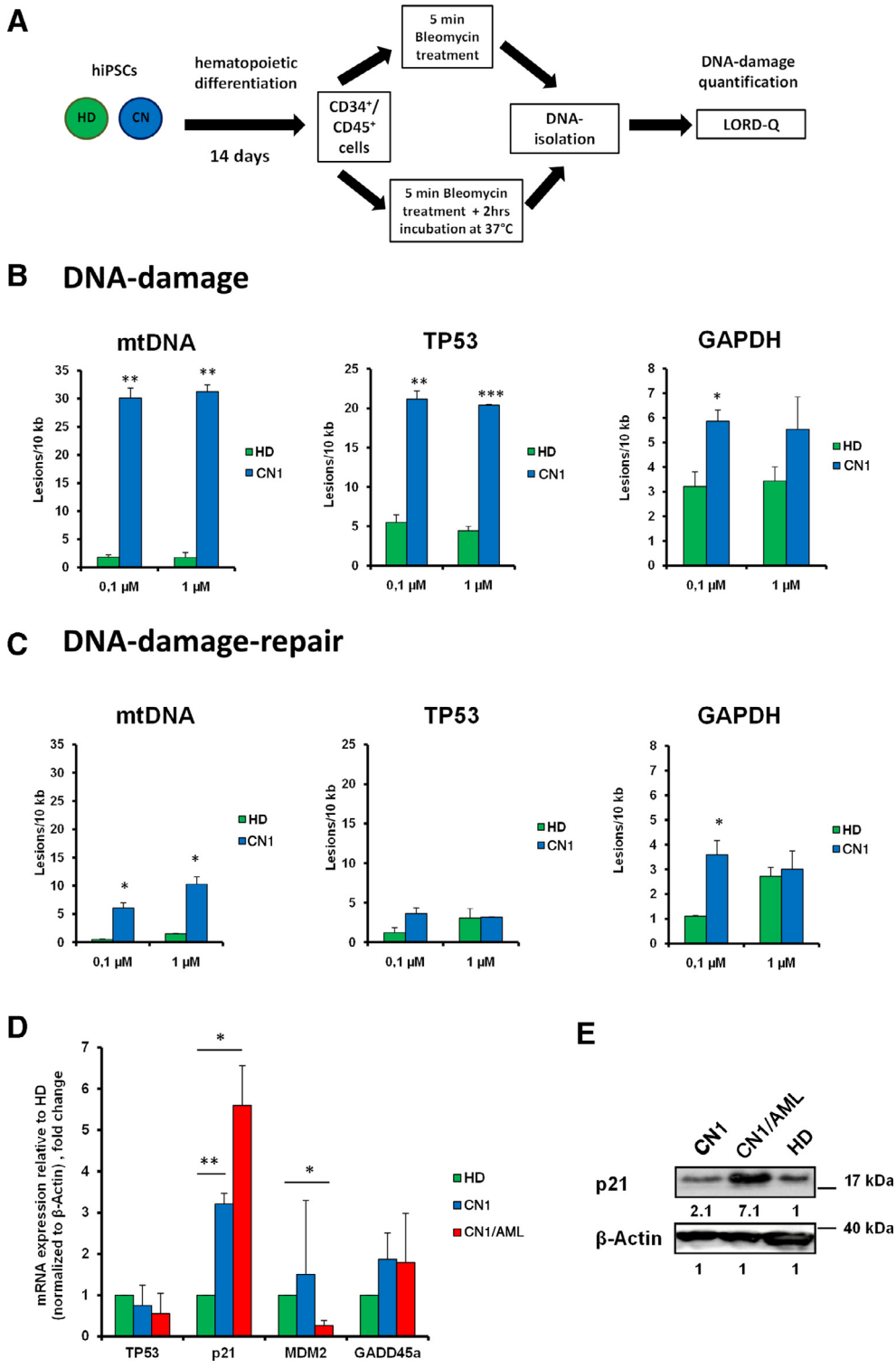

Figure 3. Quantification of DNA damage and p21 expression in $CD34^+$ and $CD45^+$ cells derived from patient-specific iPSCs. **(A)** Scheme for DNA damage measurements in HD- and CN-iPSCs derived $CD34^+CD45^+$ cells. **(B,C)** Measurement of DNA damage loci for mitochondrial DNA (mtDNA) and DNA of *TP53* or *GAPDH* gene loci of CN-iPSC-derived $CD45^+CD34^+$ cells upon 5-min treatment with 0.1 and 1 μmol/L bleomycin. DNA lesions were assessed directly 5 min (DNA damage **(B)**) and 2 hours (DNA repair **(C)**) after bleomycin treatment. Data are shown as means ± SD from two independent experiments. $*p < 0.05$, $**p < 0.01$, $***p < 0.001$. **(D)** qRT-PCR analysis of selected genes in $CD45^+CD34^+$ cells generated from different iPSCs clones on day 14 of iPSC differentiation. mRNA expression of target genes was normalized to β-actin and shown relative to HD. Data represent means ± SD from two independent experiments. $*p < 0.05$, $**p < 0.01$, $***p < 0.001$. **(E)** Representative Western blot images of p21 protein and -actin expression in $CD45^+$ cells at day 28 of iPSC differentiation. Numbers below the Western blot images indicate protein expression levels normalized to β-actin.

proper folding and intracellular localization of mutated NE is severely affected in myeloid cells of *ELANE*-CN patients. These defects ultimately lead to activation of the UPR and ER stress. We detected no activation of ATF6 and BiP in CN/AML cells compared with CN cells. These differences may be attributable to a dosage effect of mutated NE or additional coregulation of ATF4, but not ATF6, by mutated *RUNX1* and trisomy 21. Interestingly, elevated expression of ATF4 is associated with resistance to current chemotherapeutic drugs [33] and we detected hyperactivation of ATF4 in CN/AML cells. We have recently reported activation of different UPR pathways depending on the type of *ELANE* mutation [22]. Consistent with this, we demonstrate here that *ELANE* mutant p.C151Y induces expression of ATF4, ATF6, and CHOP, but not BiP. At the same time, p.G214R *ELANE* mutation caused upregulation of BiP, ATF4, and CHOP, but not ATF6. The impact of inherited CN-associated mutations (e.g., in *ELANE*) and UPR activation on leukemic progression is still unclear. It has been shown that induction of ER stress protects gastric cancer cells against apoptosis [34]. It is also known that activation of the UPR remodels the sensitivity of tumor cells to chemotherapeutic agents, making them more sensitive in some cases and more resistant in others [35]. Interestingly, upon ER stress, ATF4 is activated in mouse HSPCs, but not in more committed progenitors, leading to apoptosis of HSPCs [36]. Elevated levels of mutated NE, which we detected in $CD45^+$ cells derived from CN-iPSCs and CN/AML-iPSCs, may further amplify the UPR, and additional signaling pathways (e.g., hyperactivated STAT5a [18] or mutated *RUNX1* [37]) may protect these cells from apoptosis, resulting in leukemogenic transformation of these cells. Because *ELANE* expression is regulated by RUNX1 [38], it will be interesting to determine how missense *RUNX1* mutations affect *ELANE* expression. Cai et al. demonstrated an attenuated UPR in HSPCs from *Runx1*$^{-/-}$ mice [39] and another study showed induction of UPR by trisomy 21 in immortalized lymphocytes and fibroblasts of Down syndrome patients [40]. The induction of UPR and ER stress in HSPCs of these patients has not yet been studied, but it is known that individuals with Down syndrome often develop AML.

We identified an increased susceptibility of CN $CD34^+$ $CD45^+$ cells to DNA damage, a finding consistent with the observed prolongation in DNA repair. Interestingly, ER stress suppresses DNA double-strand break repair in tumor cells [41]. Moreover, Nagelkerle et al. demonstrated that the UPR increases the resistance of tumor cells to therapeutic agents by regulating the DNA damage response [42]. In CN patients with inherited *ELANE* mutations, a permanent stress response caused by a chronically elevated UPR may cause genotoxic stress, increasing the susceptibility of HSPCs to secondary leukemia-causing events, although the complete pathomechanism remains to be investigated. An evaluation of the expression levels of the main players in p53 signaling, a classical DNA damage response pathway, revealed strong upregulation of p21 mRNA levels, but not p53 mRNA expression, in CN and CN/AML $CD34^+$ cells. p21 protein expression was also elevated in $CD45^+$ cells of CN/AML patients compared with CN and HD-derived cells. The mechanism of p21 upregulation in CN and CN/AML cells remains to be investigated, but may be explained by increased p53 protein stability or diminished levels of the p53 ubiquitin E3 ligase MDM2. Another possibility is p53-independent activation of p21 expression. In this context, Galanos et al. reported p53-independent upregulation of p21 selectively in more aggressive tumor cells, which featured increased genomic instability, aggressiveness, and chemoresistance [43]. Unaffected expression of GADD45a, another p53 target, also argues for possibly inactive p53 and thus a p53-independent mechanism of p21 activation in $CD34^+$ cells of CN patients. Less is known about UPR-mediated regulation of p21 expression. One study described inhibition of p21 expression by CHOP [44], but we found that both CHOP and p21 levels were elevated in CN and CN/AML $CD34^+$ and $CD45^+$ cells. It is known that accumulated cytoplasmic p21 exerts anti-apoptotic functions in AML cells [45,46] and high p21 levels are associated with chemoresistance in AML [47]. Elevated expression of p21 in preleukemic cells of CN patients may make these cells resistant to apoptosis, leading to an increase in their survival and an increased probability of their leukemogenic transformation. AML blasts of CN patients are resistant to conventional chemotherapy, so bone marrow transplantation is the only treatment option in these patients [1].

Taken together, our findings demonstrate that the iPSC-based model established here is a reliable in vitro model for studying defective signaling systems underlying impaired hematopoietic differentiation in patients with bone marrow failure syndromes (in our case, CN). This model may also be used for drug development or generation of isogenic iPSC lines using CRISPR/Cas9-mediated correction of inherited disease-causing mutations.

Acknowledgments

This work was supported by the Excellence Initiative of the Faculty of Medicine, University of Tuebingen (JS), the Jose Carreras Leukemia Foundation (JS, BD), Madeleine Schickedanz Kinderkrebsstiftung (JS, MK), the Deutsche Forschungsgemeinschaft (JS, MK), the Medical Faculty of the Tübingen University (intramural Fortüne funding to M.K.), the German–Israeli Foundation for Scientific Research and Development (KW, AZ, BD), the German Cancer Consortium (KS-O, JS, PM), and the Fritz Thyssen Foundation (B.D.).

Author contributions

JS and BD made initial observations, designed the experiments, and analyzed the data; BD performed the main experiments, generated, characterized, cultured, and differentiated human iPSCs, and performed FACS, qRT-PCRs, and WBs; BO differentiated iPSCs and performed FACS; PM conducted LORD-Q experiments; AZ with the help of NL and TM established iPSC generation and EB-based hematopoietic differentiation in the laboratory; RB assisted in iPSC culture and qRT-PCR; KS-O assisted with LORD-Q experiments and provided insightful comments; CZ and KW provided patient material; LK provided insightful comments; and KW and JS supervised and supported the study and wrote the manuscript (with the help of BD).

References

1. Skokowa J, Dale DC, Touw IP, Zeidler C, Welte K. Severe congenital neutropenias. Nat Rev Dis Primers. 2017;3:17032.
2. Skokowa J, Germeshausen M, Zeidler C, Welte K. Severe congenital neutropenia: inheritance and pathophysiology. Curr Opin Hematol. 2007;14:22–28.
3. Dale DC, Person RE, Bolyard AA, et al. Mutations in the gene encoding neutrophil elastase in congenital and cyclic neutropenia. Blood. 2000;96:2317–2322.
4. Klein C, Grudzien M, Appaswamy G, et al. HAX1 deficiency causes autosomal recessive severe congenital neutropenia (Kostmann disease). Nat Genet. 2007;39:86–92.
5. Triot A, Järvinen PM, Arostegui JI, et al. Inherited biallelic CSF3R mutations in severe congenital neutropenia. Blood. 2014;123:3811–3817.
6. Klimiankou M, Klimenkova O, Uenalan M, et al. GM-CSF stimulates granulopoiesis in a congenital neutropenia patient with loss-of-function biallelic heterozygous CSF3R mutations. Blood. 2015;126:1865–1867.
7. Boztug K, Järvinen PM, Salzer E, et al. JAGN1 deficiency causes aberrant myeloid cell homeostasis and congenital neutropenia. Nat Genet. 2014;46:1021–1027.
8. Boztug K, Appaswamy G, Ashikov A, et al. A syndrome with congenital neutropenia and mutations in G6PC3. N Engl J Med. 2009;360:32–43.
9. Makaryan V, Rosenthal EA, Bolyard AA, et al. UW Center for Mendelian Genomics. TCIRG1-associated congenital neutropenia. Hum Mutat. 2014;35:824–827.
10. Makaryan V, Zeidler C, Bolyard AA, et al. The diversity of mutations and clinical outcomes for ELANE-associated neutropenia. Curr Opin Hematol. 2015;22:3–11.
11. Welte K, Dale D. Pathophysiology and treatment of severe chronic neutropenia. Ann Hematol. 1996;72:158–165.
12. Welte K, Zeidler C, Dale DC. Severe congenital neutropenia. Semin Hematol. 2006;43:189–195.
13. Skokowa J, Cario G, Uenalan M, et al. LEF-1 is crucial for neutrophil granulocytopoiesis and its expression is severely reduced in congenital neutropenia. Nat Med. 2006;12:1191–1197.
14. Skokowa J, Welte K. LEF-1 is a decisive transcription factor in neutrophil granulopoiesis. Ann N Y Acad Sci. 2007;1106:143–151.
15. Skokowa J, Welte K. Dysregulation of myeloid-specific transcription factors in congenital neutropenia. Ann N Y Acad Sci. 2009;1176:94–100.
16. Skokowa J, Welte K. Defective G-CSFR signaling pathways in congenital neutropenia. Hematol Oncol Clin North Am. 2013;27:75–88. viii.
17. Rauprich P, Kasper B, Tidow N, Welte K. The protein tyrosine kinase JAK2 is activated in neutrophils from patients with severe congenital neutropenia. Blood. 1995;86:4500–4505.
18. Gupta K, Kuznetsova I, Klimenkova O, et al. Bortezomib inhibits STAT5-dependent degradation of LEF-1, inducing granulocytic differentiation in congenital neutropenia CD34(+) cells. Blood. 2014;123:2550–2561.
19. Skokowa J, Lan D, Thakur BK, et al. NAMPT is essential for the G-CSF-induced myeloid differentiation via a NAD(+)-sirtuin-1-dependent pathway. Nat Med. 2009;15:151–158.
20. Cario G, Skokowa J, Wang Z, et al. Heterogeneous expression pattern of pro- and anti-apoptotic factors in myeloid progenitor cells of patients with severe congenital neutropenia treated with granulocyte colony-stimulating factor. Br J Haematol. 2005;129:275–278.
21. Klimenkova O, Ellerbeck W, Klimiankou M, et al. A lack of secretory leukocyte protease inhibitor (SLPI) causes defects in granulocytic differentiation. Blood. 2014;123(8):1239–1249.
22. Nustede R, Klimiankou M, Klimenkova O, et al. ELANE mutant-specific activation of different UPR pathways in congenital neutropenia. Br J Haematol. 2016;172:219–227.
23. Nanua S, Murakami M, Xia J, et al. Activation of the unfolded protein response is associated with impaired granulopoiesis in transgenic mice expressing mutant Elane. Blood. 2011;117:3539–3547.
24. Grenda DS, Murakami M, Ghatak J, et al. Mutations of the ELA2 gene found in patients with severe congenital neutropenia induce the unfolded protein response and cellular apoptosis. Blood. 2007;110:4179–4187.
25. Morishima T, Watanabe K, Niwa A, et al. Genetic correction of HAX1 in induced pluripotent stem cells from a patient with severe congenital neutropenia improves defective granulopoiesis. Haematologica. 2014;99:19–27.
26. Nayak RC, Trump LR, Aronow BJ, et al. Pathogenesis of ELANE-mutant severe neutropenia revealed by induced pluripotent stem cells. J Clin Invest. 2015;125:3103–3116.
27. Hiramoto T, Ebihara Y, Mizoguchi Y, et al. Wnt3a stimulates maturation of impaired neutrophils developed from severe congenital neutropenia patient-derived pluripotent stem cells. Proc Natl Acad Sci U S A. 2013;110:3023–3028.
28. Pittermann E, Lachmann N, MacLean G, et al. Gene correction of HAX1 reversed Kostmann disease phenotype in patient-specific induced pluripotent stem cells. Blood Adv. 2017;1:903–914.
29. Lehle S, Hildebrand DG, Merz B, et al. LORD-Q: a long-run real-time PCR-based DNA-damage quantification method for nuclear and mitochondrial genome analysis. Nucleic Acids Res. 2014;42:e41.
30. Lachmann N, Ackermann M, Frenzel E, et al. Large-scale hematopoietic differentiation of human induced pluripotent stem cells provides granulocytes or macrophages for cell replacement therapies. Stem Cell Reports. 2015;4:282–296.
31. Bonilla MA, Dale D, Zeidler C, et al. Long-term safety of treatment with recombinant human granulocyte colony-stimulating factor (r-metHuG-CSF) in patients with severe congenital neutropenias. Br J Haematol. 1994;88:723–730.
32. Germeshausen M, Skokowa J, Ballmaier M, Zeidler C, Welte K. G-CSF receptor mutations in patients with congenital neutropenia. Curr Opin Hematol. 2008;15:332–337.
33. Ye J, Koumenis C. ATF4, an ER stress and hypoxia-inducible transcription factor and its potential role in hypoxia tolerance and tumorigenesis. Curr Mol Med. 2009;9:411–416.
34. Feng R, Zhai WL, Yang HY, Jin H, Zhang QX. Induction of ER stress protects gastric cancer cells against apoptosis induced by cisplatin and doxorubicin through activation of p38 MAPK. Biochem Biophys Res Commun. 2011;406:299–304.
35. Mann MJ, Hendershot LM. UPR activation alters chemosensitivity of tumor cells. Cancer Biol Ther. 2006;5:736–740.

36. van Galen P, Kreso A, Mbong N, et al. The unfolded protein response governs integrity of the haematopoietic stem-cell pool during stress. Nature. 2014;510:268–272.
37. Skokowa J, Steinemann D, Katsman-Kuipers JE, et al. Cooperativity of RUNX1 and CSF3R mutations in severe congenital neutropenia: a unique pathway in myeloid leukemogenesis. Blood. 2014;123:2229–2237.
38. Lausen J, Liu S, Fliegauf M, Lübbert M, Werner MH. ELA2 is regulated by hematopoietic transcription factors, but not repressed by AML1-ETO. Oncogene. 2006;25:1349–1357.
39. Cai X, Gao L, Teng L, et al. Runx1 deficiency decreases ribosome biogenesis and confers stress resistance to hematopoietic stem and progenitor cells. Cell Stem Cell. 2015;17:165–177.
40. Aivazidis S, Coughlan CM, Rauniyar AK, et al. The burden of trisomy 21 disrupts the proteostasis network in Down syndrome. PLoS One. 2017;12:e0176307.
41. Yamamori T, Meike S, Nagane M, Yasui H, Inanami O. ER stress suppresses DNA double-strand break repair and sensitizes tumor cells to ionizing radiation by stimulating proteasomal degradation of Rad51. FEBS Lett. 2013;587:3348–3353.
42. Nagelkerke A, Bussink J, van der Kogel AJ, Sweep FC, Span PN. The PERK/ATF4/LAMP3-arm of the unfolded protein response affects radioresistance by interfering with the DNA damage response. Radiother Oncol. 2013;108:415–421.
43. Galanos P, Vougas K, Walter D, et al. Chronic p53-independent p21 expression causes genomic instability by deregulating replication licensing. Nat Cell Biol. 2016;18:777–789.
44. Mihailidou C, Papazian I, Papavassiliou AG, Kiaris H. CHOP-dependent regulation of p21/waf1 during ER stress. Cell Physiol Biochem. 2010;25:761–766.
45. Schepers H, Geugien M, Eggen BJ, Vellenga E. Constitutive cytoplasmic localization of p21(Waf1/Cip1) affects the apoptotic process in monocytic leukaemia. Leukemia. 2003;17:2113–2121.
46. Abbas T, Dutta A. p21 in cancer: intricate networks and multiple activities. Nat Rev Cancer. 2009;9:400–414.
47. Zhang W, Kornblau SM, Kobayashi T, Gambel A, Claxton D, Deisseroth AB. High levels of constitutive WAF1/Cip1 protein are associated with chemoresistance in acute myelogenous leukemia. Clin Cancer Res. 1995;1:1051–1057.